Progress In Electromagnetics Research Letters, Vol. 61, 125–130, 2016

A Planar End-Fire Antenna with Wide Beamwidth for 60 GHz Applications

Rongda Wang[1], Peng Gao[1, *], Peng Wang[1], and Kai Kang[2]

Abstract—A novel 60 GHz end-fire antenna for point-to-multipoint applications is presented. The prototype of this antenna is a dipole structure with a wide beamwidth. Then, the radiators are tilted with the ground is also modified to improve its directive gain while maintaining wide signal coverage. The antenna has a compact size of 10 mm × 7 mm × 0.254 mm. Measured results show that the antenna has favorable properties of 3-dB beamwidth up to 150° at 60 GHz, S_{11} less than −10 dB and stable gain of 5.9 to 6.8 dBi over 57 to 64 GHz, where these characteristics denote it fitting for 60 GHz wireless communication systems.

1. INTRODUCTION

High data rate communications for wireless personal area network (WPAN) have attracted huge attention in the past few years. With an available bandwidth of 7 GHz, the 60 GHz techniques are promising for industrial, scientific and medical (ISM) short-range communications [1]. However, compared to previously used RF bands, signals at such frequency incur high loss due to the oxygen absorption [2]. Many techniques for gain enhancement of 60 GHz antennas have been reported, such as embedding metamaterial structures [3, 4], adopting antenna array configuration [5, 6], and adding parasitic patches [7]. Yet most of them only provide narrow beamwidth, which restricts them to point-to-point applications. By using microstrip array antennas, 3.6 GHz impedance bandwidth, high gain characteristic and a 3-dB beamwidth over 76° in E-plane are achieved at the same time [8]. In [9], two wideband antipodal tapered slot (ATS) elements are utilized to configure a fan-like structure for generating a beamwidth up to 184°. However, the antenna's gain is only 1.6 dBi at the frequency of 59 GHz. In a word, a 60 GHz antenna design for point-to-multipoint applications is attractive and challenging, which has been proposed but remains to be further studied.

Dipole antennas are considered as one of the most widely applied form of omnidirectional antennas. In this paper, a planar dipole antenna for 60 GHz WPAN is proposed. Measured results show that the designed antenna covers 57–64 GHz. With the use of tilted dipole antenna and modified ground, a wide beamwidth in H-plane and gain of 5.9 to 6.8 dBi are realized.

2. ANTENNA DESIGN

The geometry of the proposed antenna (antenna B) and its prototype (antenna A) are shown in Fig. 1, which are both designed and fabricated on a RO4350 substrate, with a thickness of 0.254 mm and relative dielectric constant of 3.66. Antenna A is a planar dipole antenna with a wide beamwidth, including radiating elements and the front microstrip line of the 1.85 mm end launch connector. The ground of microstrip line is treated as a reflector. By adjusting $L1$ and $L2$, the final simulated radiation patterns of antenna A are determined and shown in Fig. 2.

Received 19 June 2016, Accepted 28 July 2016, Scheduled 3 August 2016

* Corresponding author: Peng Gao (penggao@uestc.edu.cn).

[1] Research Institute of Electronic Science and Technology, University of Electronic Science and Technology of China, Chengdu, China.

[2] School of Electrical Engineering, University of Electronic Science and Technology of China, Chengdu, China.

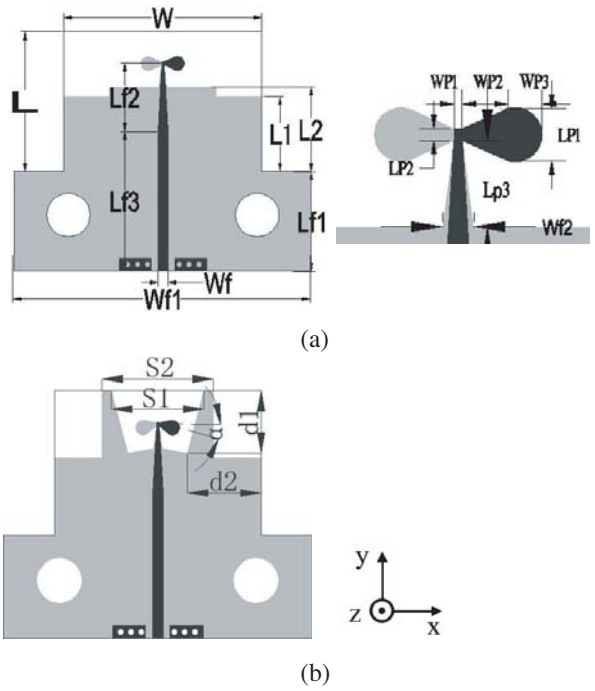

Figure 1. Geometry of: (a) Antenna A: prototype of the proposed antenna, (b) Antenna B: the proposed antenna.

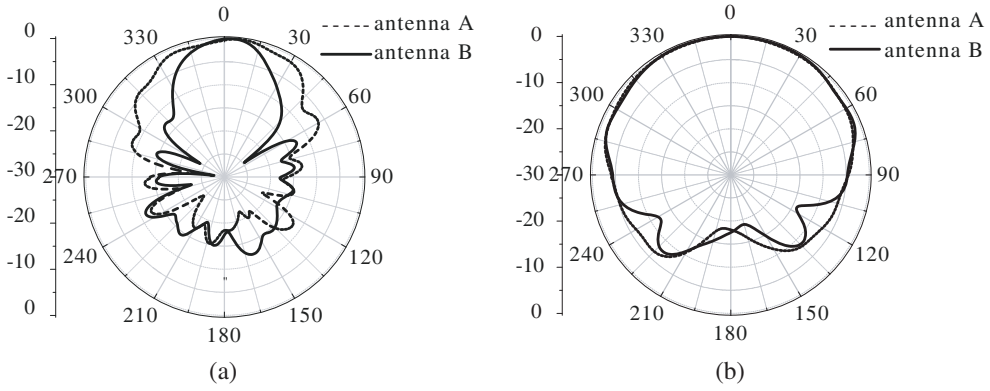

Figure 2. Simulated normalized radiation patterns at the frequency of 60 GHz: (a) E-plane, (b) H-plane.

3. GAIN ENHANCEMENT DESIGN

To enhance its directive gain while maintaining the wide beamwidth in H-plane, antenna B is proposed. As depicted in Fig. 1(b), in order to increase its directive gain, the radiators are tilted by α, and two arms extended from the ground are applied. The radiation pattern in E-plane is simulated and given in Fig. 2(a). The results show that the 3-dB beamwidth in E-plane decreases from 74° to 38°, which brings a gain enhancement of 1.8 to 2.5 dB, as plotted in Fig. 3. To maintain the beamwidth in H-plane, two triangles are removed from the ground. Fig. 2(b) shows that the simulated 3-dB beamwidth in H-plane is up to 160°. Compared with antenna A, the radiation pattern in H-plane remains almost unchanged.

The parameters are simulated and optimized by commercial software Ansoft HFSS V15. The final dimensions of the proposed antenna are set as follows: $W = 10\,\text{mm}$, $L = 7\,\text{mm}$, $Wf = 0.5\,\text{mm}$, $Wf1 = 15\,\text{mm}$, $Lf1$=5 mm, $Lf2 = 3.43\,\text{mm}$, $Lf3 = 7\,\text{mm}$, $L1 = 3.75\,\text{mm}$, $L2 = 4.2\,\text{mm}$, $Wf2 = 0.4\,\text{mm}$, $WP1 = 0.1\,\text{mm}$, $WP2 = 0.6\,\text{mm}$, $WP3 = 0.44\,\text{mm}$, $LP1 = 0.68\,\text{mm}$, $LP2 = 0.15\,\text{mm}$, $LP3 = 1.13\,\text{mm}$. $S1 = 4.5\,\text{mm}$, $S2 = 5.4\,\text{mm}$, $d1 = 3.03\,\text{mm}$, $d2 = 3.57\,\text{mm}$, $\alpha = 15°$.

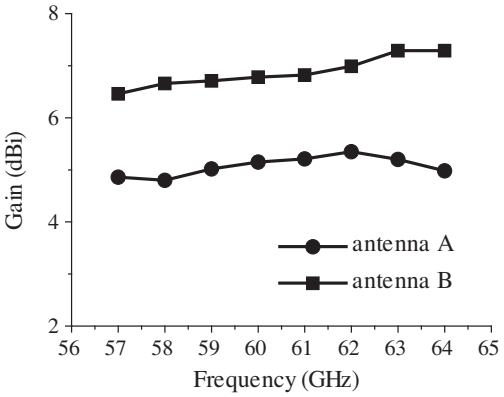

Figure 3. Simulated antenna gain.

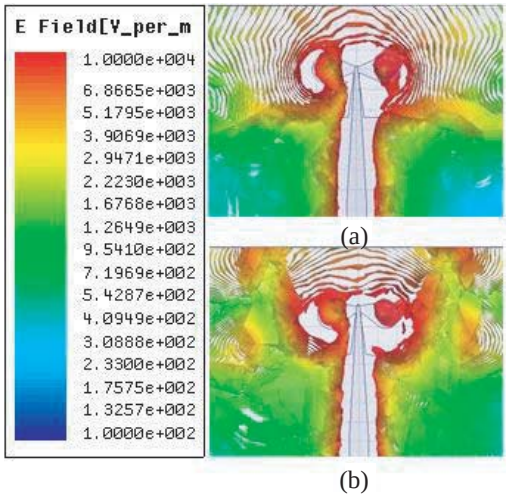

Figure 4. *E*-Field distribution of: (a) antenna A and (b) antenna B.

To explain the mechanism of antenna B, Fig. 4 shows the simulated *E*-field distribution of antenna A and antenna B, respectively. It is seen that antenna B has a more uniform aperture field distribution than antenna A, which results in a narrower beamwidth in *E*-plane.

4. ANTENNA MEASUREMENT SYSTEM

A photo of the system in lab is shown in Fig. 5. The measuring system consists of a vector network analyzer (VNA), a high sensitive spectrum analyzer (SA), and a standard horn antenna with high gain which runs back and forth on a nylon slide rail. In addition, to obtain more accurate measured results, absorbing materials are utilized to minimize the effect of nearby equipments. During the measuring process, a VNA of Agilent PNA-X N5247A is connected to the device under test (DUT) as a transmitter, and a high sensitive spectrum analyzer (SA) is connected to a standard horn as a receiver. The gain of the proposed antenna is calculated using the following equation

$$G_t(\text{dB}) = P_r(\text{dBm}) - P_t(\text{dBm}) - G_r(\text{dB}) + L_r(\text{dB}) + L_t(\text{dB}) + L_s(\text{dB}) \tag{1}$$

where G_t is the gain of DUT and G_r the gain of standard horn. P_t and P_r are the transmitting and receiving powers of SA and VNA, respectively. L_t and L_r are losses of cables and connectors in the transmitter and receiver, respectively. L_s is the loss in free space, which is calculated as

$$L_s = 20 \lg \frac{4\pi R}{\lambda} \tag{2}$$

where R is the distance between receiving and transmitting antennas, and λ is the wavelength of free space.

5. EXPERIMENTAL RESULTS AND DISCUSSION

5.1. Fabrication and Measurements

To verify the simulated results, antenna B is fabricated and measured, whose photograph is shown in Fig. 6. The *S*-parameters are measured with Agilent PAN-X N5247A vector network analyzer (VNA), with the connection to a Southwest Microwave V-band end-launch connector. Simulated and measured S-parameters are given in Fig. 7. According to measured results, over 10 dB return losses impedance bandwidth covers 57–64 GHz, which is overall in good agreement with simulations, and the small discrepancy is due to the dispersion of the connectors and fabrication errors.

5.2. Radiation Performance

The simulated and measured normalized radiation patterns of XY-plane and ZY-pane at 57 GHz, 60 GHz and 64 GHz are depicted in Fig. 8. It should be noted that due to the measuring conditions and

Figure 5. Overview of the antenna measurement system in lab.

Figure 6. Photograph of fabrication.

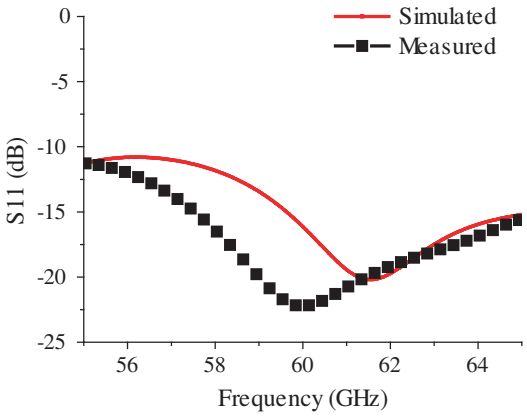

Figure 7. Simulated and measured return loss of antenna B.

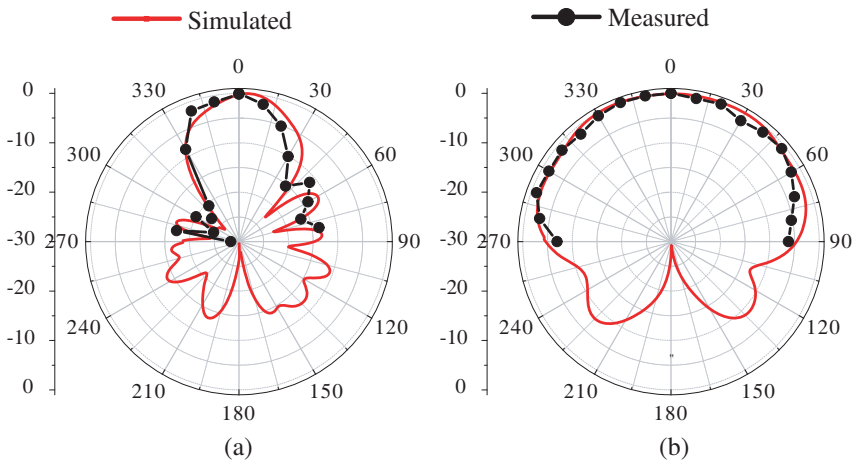

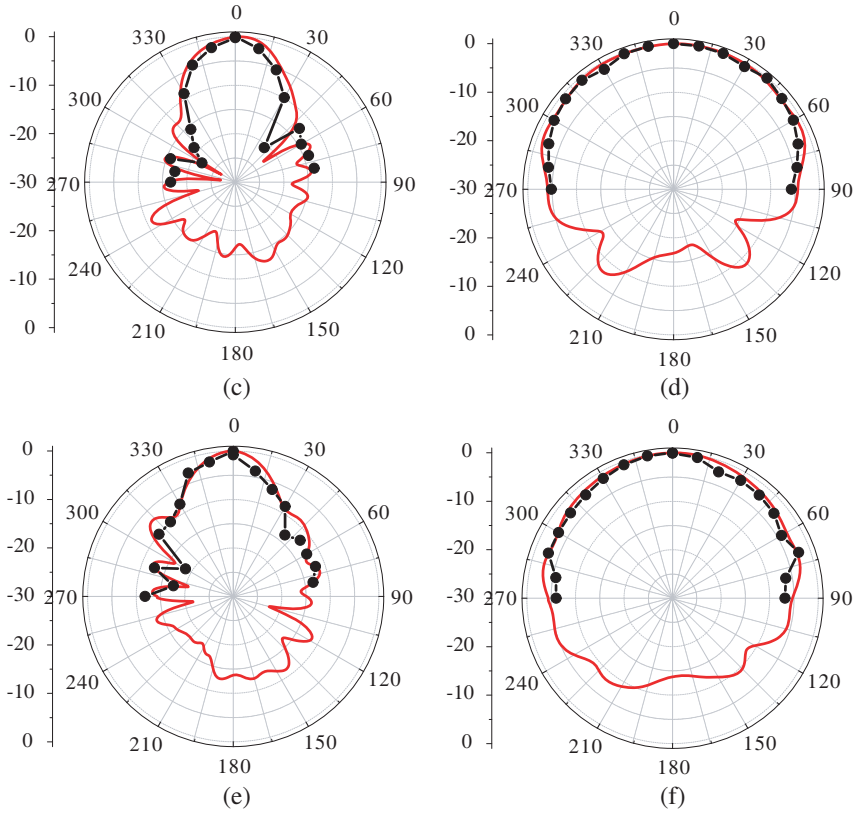

Figure 8. Simulated and measured normalized radiation patterns of antenna B: (a) 57 GHz XY-plane, (b) 57 GHz ZY-plane, (c) 60 GHz XY-plane, (d) 60 GHz ZY-plane, (e) 64 GHz XY-plane, (f) 64 GHz ZY-plane.

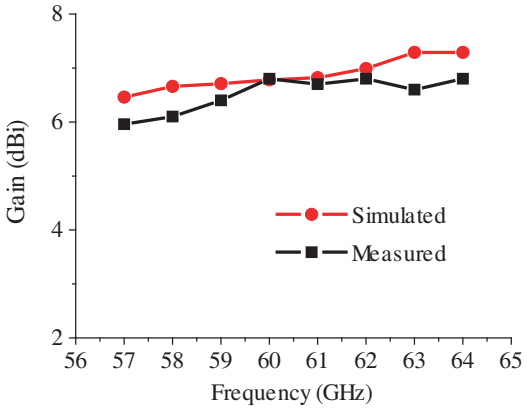

Figure 9. Simulated and Measured antenna gain of antenna B.

because the end launch connector has certain effect on back radiations, only front radiation patterns are measured and plotted. Measured results show beamwidth values of the proposed antenna have a small variation from 142° to 153° across the working band. It is also seen in Fig. 9 that the antenna has stable peak gain variation less than 1 dB, and the max peak gain is up to 6.8 dBi. These denote that this antenna can be applied in 60 GHz wireless system.

6. CONCLUSION

A novel 60 GHz antenna for point-to-multipoint applications is proposed. Its dimension is 10 mm × 7 mm × 0.254 mm. By tilting the radiators and modifying the ground, the directive gain is improved while 3-dB beamwidth remains unchanged. Measured results show that the proposed antenna has good impedance matching, wide beamwidth and steady gain from 5.9 to 6.8 dBi across 57–64 GHz. Therefore, this antenna is suitable for 60 GHz wireless applications.

REFERENCES

1. Baykas, T., C. S. Sum, Z. Lan, J. Y. Wang, M. A. Rahman, H. Harada, and S. Kata, "IEEE 802.15.3c: The first IEEE wireless standard for data rates over 1 Gb/s," *IEEE Commun. Mag.*, Vol. 49, No. 7, 114–121, 2011.
2. Park, M., C. Cordeiro, E. Perahia, et al., "Millimeter-wave multi-Gigabit WLAN: Challenges and feasibility," *IEEE 19th International Symposium on Personal, Indoor and Mobile Radio Communications*, 1–5, 2008.
3. Dadgarpour, A., B. Zarghooni, B. S. Virdee, et al., "Millimeter-wave high-gain SIW end-fire bow-tie antenna," *IEEE Transactions on Antennas & Propagation*, Vol. 63, No. 5, 2337–2342, 2015.
4. Bao, X. Y., Y. X. Guo, and Y. Z. Xiong, "60-GHz AMC-based circularly polarized on-chip antenna using standard 0.18-μm CMOS technology," *IEEE Transactions on Antennas & Propagation*, Vol. 60, No. 5, 2234–2241, 2012.
5. Wang, L., Y. X. Guo, and W. X. Sheng, "Wideband high-gain 60-GHz LTCC L-probe patch antenna array with a soft surface," *IEEE Transactions on Antennas & Propagation*, Vol. 61, No. 4, 1802–1809, 2013.
6. Liu, W., Z. N. Chen, and X. Qing, "60-GHz thin broadband high-gain LTCC metamaterial-mushroom antenna array," *IEEE Transactions on Antennas & Propagation*, Vol. 62, No. 9, 4592–4601, 2014.
7. Chin, K. S., W. Jiang, W. Che, et al., "Wideband LTCC 60-GHz antenna array with a dual-resonant slot and patch structure," *IEEE Transactions on Antennas & Propagation*, Vol. 62, No. 1, 174–182, 2014.
8. Biglarbegian, B., M. Fakharzadeh, D. Busuioc, et al., "Optimized microstrip antenna arrays for emerging millimeter-wave wireless applications," *IEEE Transactions on Antennas & Propagation*, Vol. 59, No. 5, 1742–1747, 2013.
9. Sun, M., X. Qing, and Z. N. Chen, "60-GHz end-fire fan-like antennas with wide beamwidth," *IEEE Transactions on Antennas & Propagation*, Vol. 61, No. 4, 1616–1622, 2013.